https://dx.doi.org/10.4314/dujopas.v9i4a.2
ISSN (Print): 2476-8316
ISSN (Online): 2635-3490
Dutse Journal of Pure and Applied Sciences (DUJOPAS), *Vol. 9 No. 4a December 2023*

Lineaments Characterization and their Tectonic Significance in Mineralization using Landsat TM Data and Field Studies along Mambilla Plateau, Northeast, Nigeria.

Yohanna Andarawus[1]* Othniel Kamfani Likkason[2], Maigari Abubakar Sadiq[3], Ali Sani[2] Mohammed Kaura Aliyu[1] and Ibrahim Yusuf Anzaku[1]

[1]Department of Geology,
Federal University of Lafia,
P.M.B 146,
Nasarawa State,
Nigeria

[2]Department of Physics,
Abubakar Tafawa Balewa University Bauchi,
P.M.B 0248,
Bauchi State,
Nigeria

[3]Department of Applied Geology,
Abubakar Tafawa Balewa University Bauchi,
P.M.B 0248,
Bauchi State,
Nigeria

***Correspondence's email:** sarkikubong@gmail.com,
yohana.andarawus@science.fulafia.edu.ng

Abstract

Lineament characterization and their tectonic significance in mineralization using Landsat TM data and field studies Along the Mambilla Plateau and environs, northeast Nigeria .The area forms part of the mineralized shear zone of the Northeastern, part of the Basement Complex. The Basement Complex rocks underlie more than two-thirds of the plateau and date back to the Precambrian to early Paleozoic eras. While the remaining part of the plateau and its surroundings are made up of volcanic rocks of the upper Cenozoic to Tertiary and Quaternary ages. Remote sensing imagery data and field measurements were integrated for mapping the structural elements and hydrothermal alteration zones related to mineralization. Tectonically the lineaments trends NE-SW, NNW-SSE, NW-SE, and NS, are the main trends controlling mineralization in the area based on data from remote sensing and field measurements. On the other hand, applying band ratios and the constrained energy minimization (CEM) technique to Landsat-8 data pointed out alteration minerals associated with the hydrothermal fluids. Silica, sericite, and chlorite are the common alteration minerals detected, while goethite and epidote are less common in the alteration zones of the area under study. A combination of CET structural complexity, circular features, and alteration zones produced a potential mineralization map, pointing out numerous prospective zones for mineralization that are proximate to areas where artisanal

**Author for Correspondence*

mining activities are carried out. The predictive map was validated by projecting the known prospect zones in the study area, reflecting an agreement between the known occurrences and the higher classes of the predictive zone. The techniques in the current research can be adopted as a direct indicator for structural mapping and detecting alteration zones related to mineralization elsewhere.
Key words: Remote, Sensing, Lineaments, Structures, Mineralization

INTRODUCTION

With the advances in remote sensing technology over the last decades, remote sensing data integration, also known as data fusion and data merging, has become a powerful tool for both visual and digital image interpretation. This is a process whereby data with different spatial and/or spectral characteristics over the same region are processed and evaluated in a single red-green-blue (RGB) color combination image. This technique has primarily been applied to improve poor spatial resolution multi-spectral optical remote sensing data with higher spatial resolution panchromatic data (Daily *et al*., 1979; Carper *et al*., 1990; Franklin and Blodgett, 1993). Many studies have been conducted to integrate the 30 m spatial resolution Landsat Thematic Mapper (TM) data with the 10 m spatial resolution Satellite Pour l' Observation de la Terre (SPOT) data for addressing geological problems (Daily *et al*., 1979; Papathanassiou and Buchroithner, 1993; Pradhan *et al*., 2010). Data integration can also be effective in combining remote sensing datasets that have comparable spatial resolutions yet measure different properties of the imaged terrain. This includes, but is not limited to, the integration of multi-spectral optical remote sensing data with radar data (Pradhan *et al*., 2008; Buchroithner, 2002). Multi-spectral optical remote sensing data record information based on material composition, whereas radar data emphasize surface roughness and morphology. Hence, the integration of these datasets allows the display and analysis of the two properties in a single RGB color combination image. In addition, the introduction of digital elevation models (DEMs) adds the element of three-dimensionality that is important in the analysis of many geological features, such as morphologically defined structures and lava flows of different generations.

The objectives of this work include demonstrating the usefulness of remote sensing and field measurements in structural analysis of the Basement Complex rocks. To demonstrate how remote sensing data and field measurement integration can be used for mapping lithological units and morphologically defined geological features. The Mambilla Plateau and environs are ideal for demonstrating the effectiveness of data integration due to the lack of vegetation and soil cover and the almost continuous exposure of bedrocks. They are also known for their artisanal mining activities.

STUDY AREA LOCATION, GEOLOGICAL SETTING AND GEOMORPHOLOGY

The study area is basically part of the Sardauna and Gashaka Local Government Areas of Taraba State, Northeastern Nigeria. It is located between latitudes 6°30′ 00 N to 7°30' 00 N and longitudes 11° 00' 00 E to 11° 30' It is located between latitudes 6° 30' 00'' N to 7° 30' 00'' N and longitudes 11° 00' 00 E to 11° 30' 00'' E, having a total land mass of 6,050 km^2, and forms the southernmost tip of the eastern part of the northern part of Nigeria (Tukur *et al.,* 2005) (Fig. 1). This plateau is Cameroon-locked in the southern, eastern, and western parts (Frantz, 1981). According to Mubi and Tukur (2005), the Basement Complex rocks underlay more than two-thirds of the plateau and date back to the Precambrian to early Paleozoic Era. Meanwhile, according to Jeje (1983), the remaining part of the plateau and its surroundings is made up of volcanic rocks of the upper Cenozoic to Tertiary and Quaternary ages. The volcanic rocks

originated from basalt flows extruded from fissures in tectonic lines. The volcanic rocks are of the basaltic suite: olivine basalt and trachyte basalt. The plateau has its south and eastern escarpments standing along the Cameroonian border, while the remainder of its northern escarpment and its western slope are in Nigeria.

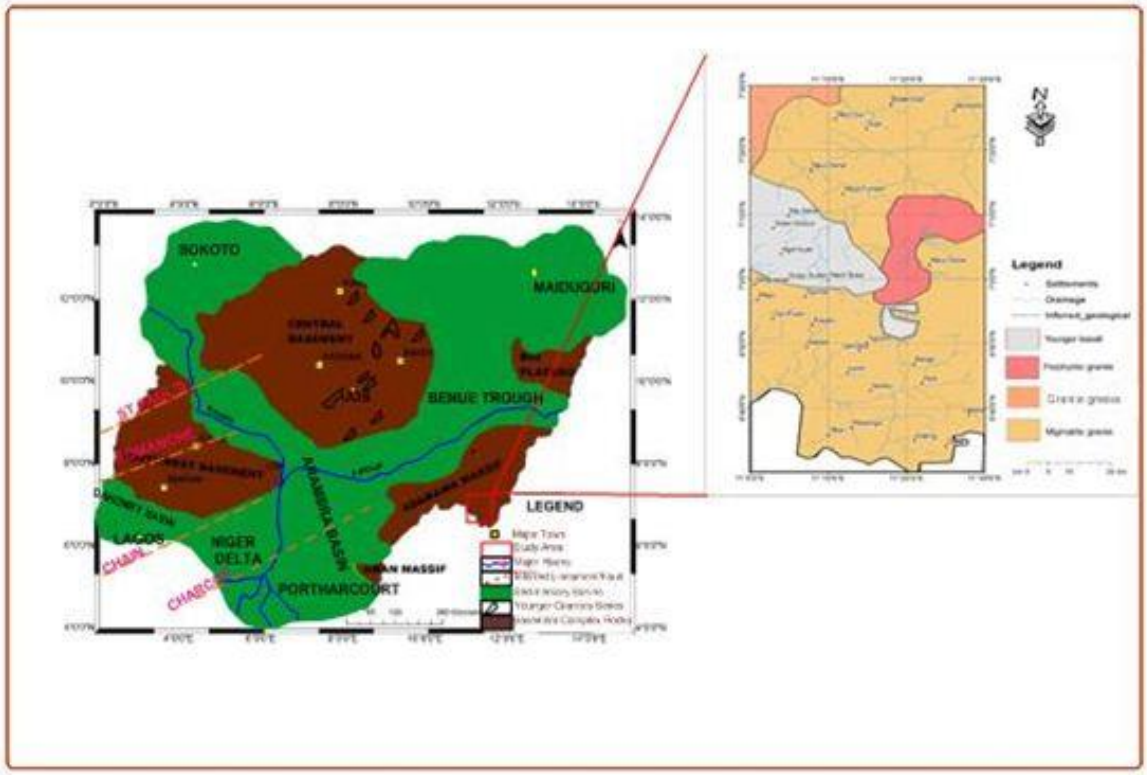

Figure 1: Structural map of Nigeria showing rocks distribution and the prominent fracture zones in Nigeria(Modified after Udensi *et al.,* 2003).

MATERIALS AND METHODS

Remote Sensing Imagery Data

Two Landsat-8 images acquired on July 7, 2020, and September 30, 2020, were used. They contain the Operational Land Imager (OLI) sensors (Roy *et al.*, 1998). OLI provides data from nine spectral bands, giving resolution imagery from 15 m for the panchromatic band to 100 m for the thermal infrared spectrums, and the visible and shortwave infrared reflect 30m spatial resolution (http://earthexplorer.usgs.gov). The obtained data was exposed to several preprocessing steps such as geometric projection, atmospheric correction, spatial resolution merge, mosaic generation technique, and the area of interest for preparing it for advanced processing techniques by the latest versions of ArcGIS and ENVI software.

Band Ratio (BR)

The band ratio technique is of great importance in the discrimination of the different rock units and in the clarification of hydrothermal alteration zones based on the difference in the spectral signature of minerals and various rock units (Goetz *et al*., 1983). In mineral mapping, the BR technique is usually used to enhance the spectral response of the alteration minerals within the alteration zones, counting on their distinguishing absorption characteristics at specific wavelengths for every alteration mineral (Pour *et al.*, 2019). Thus, the selection of

appropriate ratios in the BR technique can lead to accurate distinctions for OH-bearing minerals and iron oxides, resulting in a composite image in RGB that can be utilized to achieve the study goal.

Constrained Energy Minimization (CEM)

Constrained Energy Minimization(CEM) was used in signal processing (Farrand and Harsanyi, 1997; Harsanyi, 1993). CEM has grown in significance and is now one of the methods most frequently employed in target abundance mapping. By treating all features other than the target as the unknown background, this strategy enhances the response of the target spectrum and suppresses all other feature responses (Nikolakopoulos *et al*., 2006). Additionally, by mapping alteration zones based on the spectral signature of alteration minerals, it lessens the need for exploratory field visits. The processing program (ENVI V.5.3) includes a USGS spectral library from which the spectral fingerprints of the minerals used in this investigation were obtained.

SRTM DEM data

Digital elevation models (DEMs), an exhaustive high-resolution digital topographic database of Earth, are the result of the multinational Shuttle Radar Topography Mission (SRTM) project (Nikolakopoulos *et al*., 2006). From the DEM data, surface lineaments can be automatically extracted (Süzen and Toprak, 1998). Lineament mapping automatically with shaded DEMs Shaded relief pictures were produced using SRTM DEM 90 m data, and these images can help with fault extraction and surficial lineaments (Ganas *et al.,* 2005). Geomatica (PCI), 2015 automatically extracts line segments using the default settings for the photos of shaded relief. After that, the output is manually modified to exclude any man-made features (buildings, roads, etc.) in order to enhance the agreement between the extracted lines and the geological characteristics.

Geological Mapping, Structural Measurements and Sample Collections

Pre-field work was the initial phase, which entails gathering pertinent published and unpublished material. Planning fieldwork, creating base maps, and interpreting thematic imagery are all included. Field work, comprising lithological description, structural measurements, and rock sample collecting, constitutes the second step. A GPS (Geographic Positioning System), plastic flagging tape, and a tiny metal tag or plastic pin-marker with the sample number on it were used to record the location and description of each sample. Representative samples were taken at several locations along veins that might bear mineralization. Samples were taken along profiles perpendicular to the prevailing direction of the buildings using a 500 m by 500 m square grid. Records were kept of attitudes of structures.

RESULTS AND DISCUSSION

Surface Structural Trend Analysis of Lineaments

The remaining uncorrelated bands are mixed in RGB, and models are generated by the False Color Composite (FCC) of bands 753 and 764 (Figure 2) based on their correlation coefficient. The lithologies and alteration zones are mapped by these two color composite models (Figure 2), which were created using Landsat-8 Mambilla and its surroundings. The textural characteristics of the outcrop rocks in the picture allow them to be identified from the surrounding region. The crystalline texture and structural features of the rocks in the image's area section are clearly seen in the bands' natural RGB color combination.

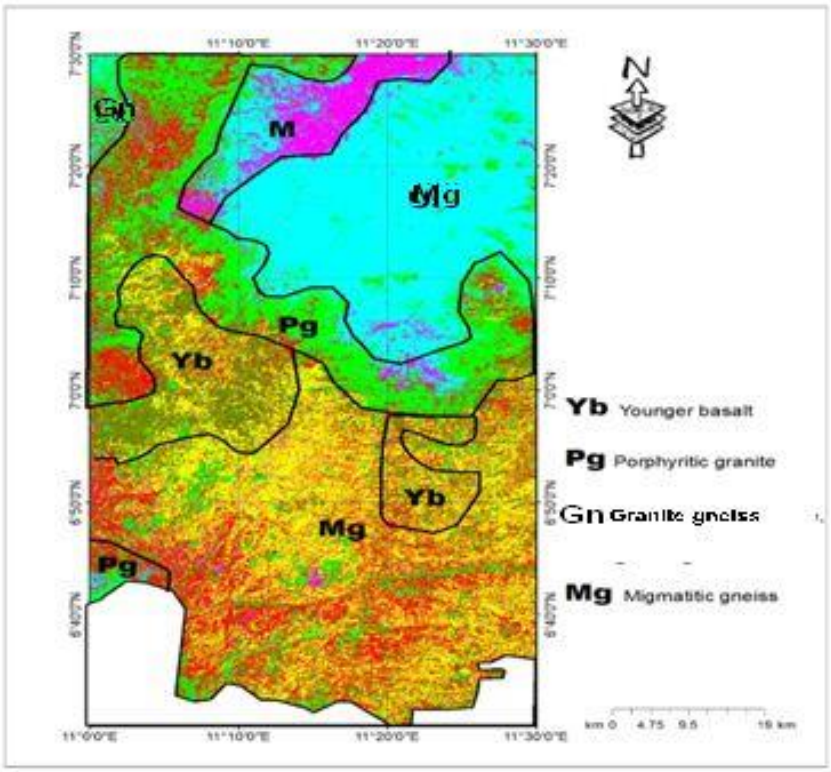

Figure 2: The false color composite image of Landsat-8 ETM+ (bands 7, 4, 2 in R, G, and B) shows the following rocks: migmatite-gneiss (Mg), granite gneiss (Gn), porphyritic granite (Pg), and younger basalt (Yb).

Principal Component Analysis (PCA)

PCA normalizes the seven OLI bands and strengthens, compresses, and confines the leading bands. (El-said et al., 2014) They were each linearly improved and presented as composite images. Bands 2456 and 716 were the PCAs employed in this investigation (Fig. 5). As shown in Fig. 5, the calculated statistical individual images and various data percentages were produced. According to the eigenvectors, the majority of the younger basalt, porphyritic granite, migmatite gneiss, and migmatite-gneiss could be distinguished from one another by their bright pixels in PC2 of PCA 2456, which has a negative absorption in band 3 (-0.434848) and a positive high reflectance in band 6 (0.451293). On the other hand, the dark pixels were representative of the undifferentiated granite, migmatite, and granite gneiss. The aforementioned rocks were also recognized as bright green, purple, yellowish, and pinkish pixels in the RGB composite of PCA 716 (Figure 3).

After the band 5 negative eigenvector value reflectance and positive in band 4, the PC of 2456 of the younger basalt, porphyritic granite, migmatite gneiss, and migmatite-gneiss were distinguished by bright pixels in PC2. This is despite the fact that the positive absorption eigenvector in band 6 (0.518572) and negative in band 4 (-0.959506) mapped dark pixels. Based on the composite of the PCA 716 image, the majority of the reddish and pinkish pixels correspond to the undifferentiated rocks of migmatite gneiss in the research area. The research area's different rock types showed a good correlation with the geological map of Mambilla and its surroundings.

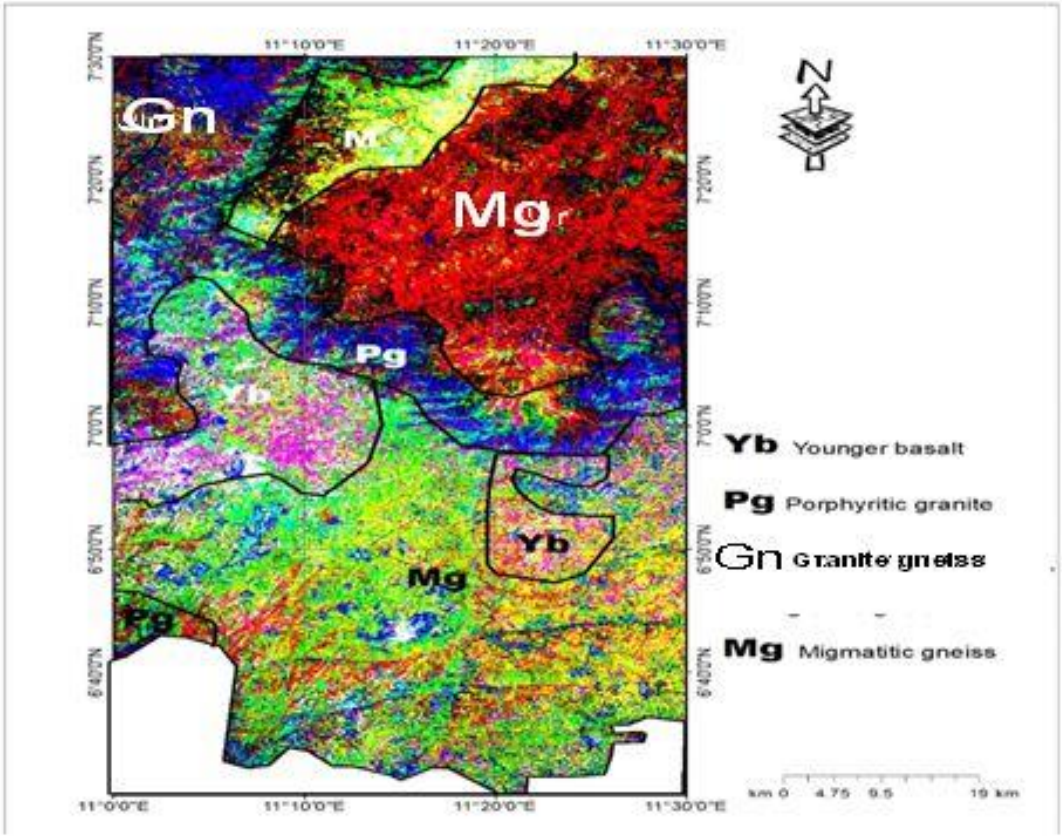

Figure 3: Principal component analysis of the study area's Landsat 8 ETM+ image (PC2, PC1, and PC4 in R, G, and B) identified the following rocks: migmatite-gneiss (Mg), granite gneiss (Gn), Porphyritic granite (Pg), and younger basalt (Yb)

Digital Image Processing

Upon processing satellite pictures (Figure 4), the principal fracturing networks at the Mambilla Plateau and its surroundings were analysed, allowing for the identification of the prevailing orientations of linear structures. A synthetic map of the lineaments was extracted using the directed filtering technique applied to the SRTM image (Figure 5). With structures primarily ranging between N80°E-80°E and N30°E/40°E, the rose diagram of the lineaments thus obtained shows two main directions in the NE-SW and NW-SE frames; we also observe two secondary directions in the NW-SE frame where the lineaments have the directions N120°E, 80°E, and N140°E/40°E. The synthetic linear map in Figure 5 was made possible by the principal component analysis method applied to the first three bands of the Landsat 8 image. The resulting rose diagram displays two secondary directions, N-S and NW-SE, after the primary direction of the lineament structures, which is NE-SW with structures ranging between N20°E and N70°E. After lineaments were recovered from the 764 OLI band composite, they were plotted into a rose diagram and shown to trend mostly in the NW-SE and NE-SW directions, with secondary trends in the NNE-SSW and NEE-SWW directions (Figure. 6). Curlinear qualities are seen in the structural control of the lineaments. They mainly displayed fractures and surface and subsurface structural faults. Elevated values of these geological formations indicate the presence of tectonics and minerals within the studied region. Major faults and fractures that might hold minerals and have mining potential were suggested by the high lineament density (Figure. 7).

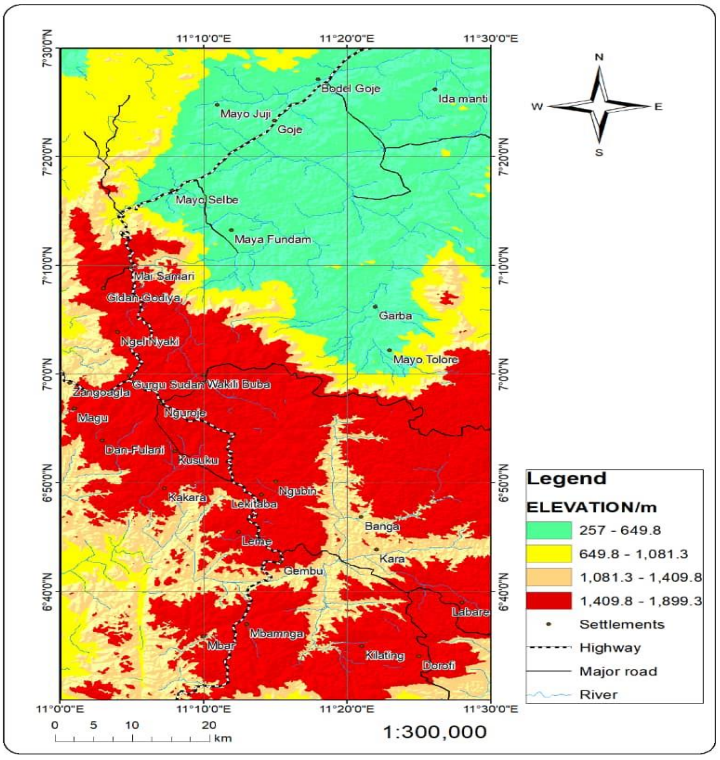

Figure 4: Digital elevation map of the study area

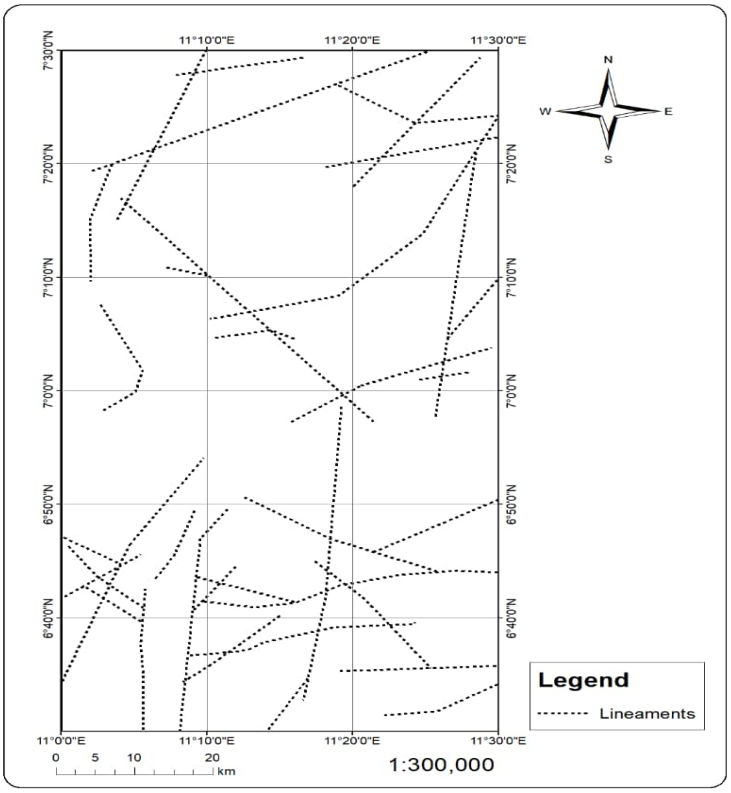

Figure 5: Structural lineaments map of the study area extracted from satellite data

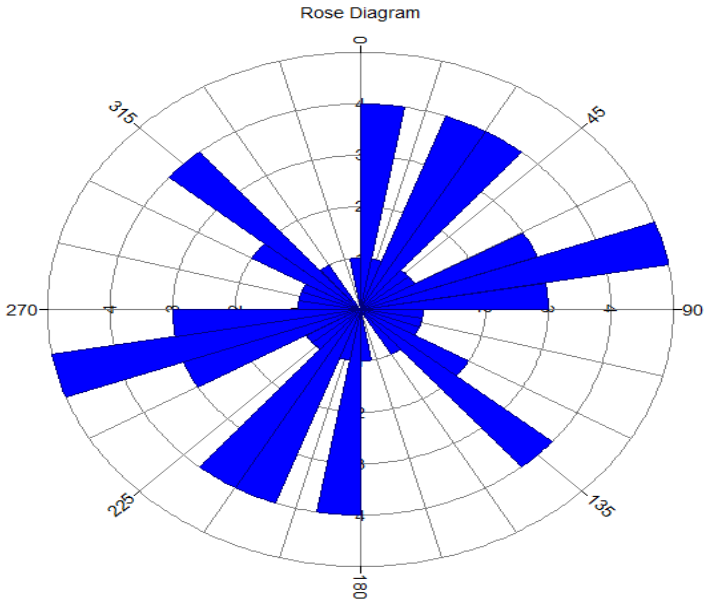

Figure 6: Rose diagram extracted from Satellite imagery

Lineament Density Map Analysis

Zones of structural density are reflected by the automatically derived surficial lineaments from the DEM data (Figure 4). High structural density is evident in the mining areas, demonstrating the value of the lineament density map in identifying prospective mineralization zones and the structures that govern mineralization (Domzalski, 1964). As may be seen in the accompanying rose diagram from satellite data (Figure 6), it displays zones of high structural complexity represented by a broad NE-SW trend (Figure 7) along with less prevalent NNW, WNW, NS, and NE tendencies. These trends and the tendencies of surficial structures are positively correlated. The following minerals—blue sapphire, aquamarine, tourmaline, amethyst, cassiterite, and bauxite—that are known to be mined in the region—such as Maisamari, Gurgu, Yelwa, Mayo Ndaga, Lekitaba, and Nguroje—have their structural complexity zones depicted (Figure 7). to confirm the effectiveness of the methods employed. Significant agreement has been seen between the main findings of this investigation and previously published field geology data. Other structures have NE-SW and E-W directions. (Abdelnasser and Kumral, 2017, Klemm and Klemm (2013) noted the NW direction as a major trend for mineralization. Mineralization at Maisamari, Gurgu, Yelwa, Mayo Ndaga, Lekitaba, and Nguroje areas follows brittle-ductile shear zones in the NE-SW direction. According to El-Desoky *et al*. (2021), mineralization extends in both NW-SE and N-S directions and is linked to structural elements including faults and shear zones. The majority of quartz veins often run N-S or NNE-SSW, while the emergence of non-mineralized quartz veins tends to trend in the NW direction, according to Helmy *et al*. (2004). The primary quartz lodes, according to Klemm & Klemm (2013), strike NE-SW, but the mined quartz veins follow a shear zone that runs NW and ENE-WSW. In addition, the lineaments maps (Figure 5) were used to construct a density map (Figure 7) that defined the structural density zone. Given current mining operations in regions with medium-to high-lineament densities (Figure 7), which shows a strong link between sites' mineralization and higher lineament densities, Klemm and Klemm (2013).

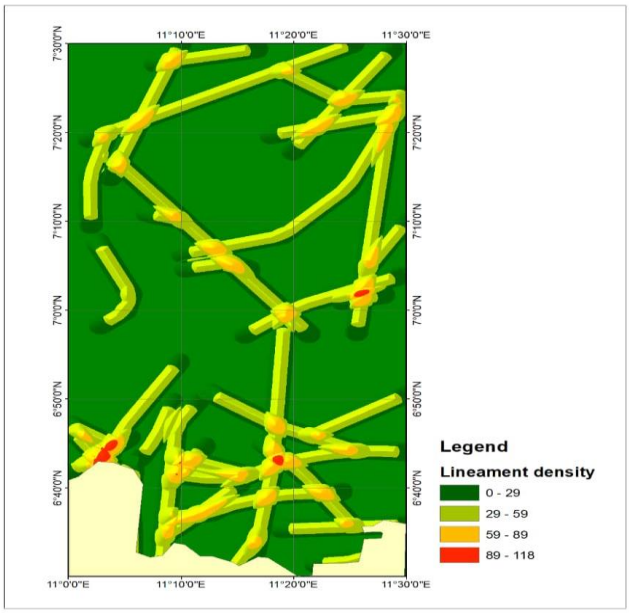

Figure 7: Lineament density map of the study area

Geology and Structural Geology of the Area

Traversing through the study area allowed for the geological surveying of the area. Younger basalts, granite porphyry, granite gneisses, and migmatite gneisses were among the lithologies found (Figure 1).

Younger Basalts

Mafic rocks, which make up this unit, are visible in the study area's western section. The predominant rock unit has a typical NE-SW strike direction and is mafic without foliation. The rocks in the area are green, brownish, and dark grey when they are fresh and aged, respectively. Their forms have evolved from rounded to subrounded and elongated. It implies that there hasn't been significant deformation of the rock. This result is consistent with the Dupreez and Barber (1995) research. Large-scale In the Mambilla region, tertiary volcanic materials are found as highland plateaus. The Mambilla Plateau is home to the tertiary basalts, which are primarily composed of widespread basalts and trachytic lavas (Dupreez and Barber, 1995). These volcanic rocks, which include olivine basalt, the basalt suite, and trachyte basalt, include mixes of quartz free minerals and amphiboles and pyroxenes (Mould, 1960).

Porphyritic Granites

In the eastern portion of the research region (At Goje and Mayo Talore), coarsely crystalline igneous rocks with a porphryritic structure were found. Large and small crystals coexist in porphyritic granites, yet they are all still very uniform in size. Primarily granitic plutonic masses. Broadly speaking, these descriptors apply throughout the entire survey area. The lithology covers about 10% of the area. This unit is the smallest lithology in the research region. It is severely fractured, trending from N-S to NE-SW (Figure 6).

The Granite-Gneiss Complex

Additionally located in the northeastern region of the research region, the granite gneiss has a significant foliation and is closely related to the migmatite gneiss. The type of rock has a medium to coarse-grained texture with colours ranging from light to dark. They have muscovite, biotite, quartz, feldspar, and weakly developed leucocratic strata. This unit, which

makes up about 8% of the study area, is a small section of the lithology that trends from north to south and is heavily foliated and broken. Gneisses are crystalline rocks with coarse grains that are banded and contain phanerictic mineral grains. Biotite is found in combination with the dark-colored mineral. The banding results from the separation of different minerals into layers that are light-colored (leucocratic) and dark-colored (melanocratic). While the light bands are made up of light-colored minerals like feldspar and quartz, the dark bands are made up of dark minerals like biotites and horneblende. The bands range in thickness from 2 mm to 2 cm.

The Migmatite-Gneiss Complex

About 60% of the study region is made up of this unit, which is the main lithology and trends from the north-south to the northeast-northwest (Table 1). It is extensively foliated and broken. Because of the intrusive bodies that are encroaching on the rocks, the foliations' degree of orientation constantly changes. There were quartz and vein-let veins many metres thick, parallel to the direction of the foliation, and frequently reorienting. The study area's surrounding migmatite gneiss is extensively foliated and banded with melanocratic (biotite and hornblende minerals) and leucocratic (feldspar and quartz) mineral layers. Brittle deformation has a strong effect on the rock, causing joints, shear zones, and fractures to occur. A few potential mineralization-hosting structures, including joints, faults, veins, and dykes, were noted in the research region.

Table 1:Some structural Readings taking on the study area

S/N	STRIKE	DIP
1	100	20SE
2	076	30SE
3	062	50SE
4	078	10SE
5	070	40SE
6	096	20SE
7	088	28SE
8	078	20NW
9	064	44NW
10	105	40SE
11	068	30SE
12	080	34SE
13	074	30SE
14	076	30SE
15	098	40SE
16	104	45SE
17	058	40NW
18	092	30SE
19	060	40SE
20	056	20SE
21	042	25NW
22	048	34NW
23	098	30NW
24	046	32NW
25	038	20SE
26	060	26SE

27	344	70SE
28	342	76SE
29	334	70SE
30	336	74SE

Fractures (Faults and Joints)

In the research region, fractures on a rock were found where there have been no discernible motions of one side in relation to the other (plates I and II). Nearly every one of the many lithological units has a junction of some kind. These are naturally occurring fractures that occur in the continuity of a rock body or layer without any discernible or quantifiable movement parallel to the fracture's surface (plane). They were trending in the NNE-SW and NNE-SSW directions. This embodies the events of the pan-African orogenic cycle. Because they may be found in practically every rock exposure, joints are among the most ubiquitous geologic formations. They occur in relatively distinct tectonic contexts and varies substantially in appearance, dimension, and organisation (Ekwueme, 1993).

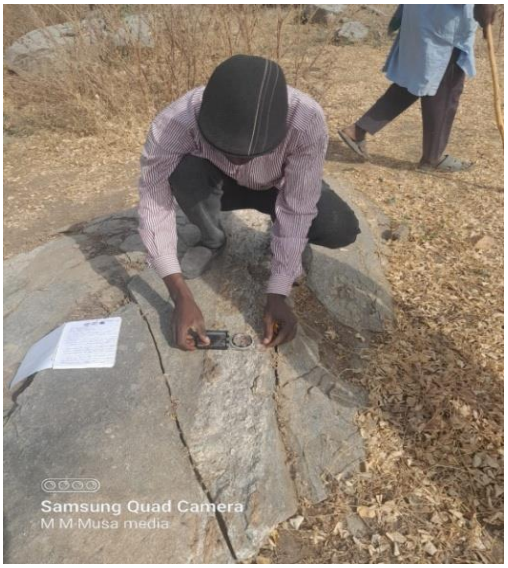

Plate I: Joints in the study area

PlateII: Vein in the study area

The research region (Plates III and IV) included fractures with rather noticeable movement, especially at Gembu, Ngoroje, and Mayo Sirte. Due to the hanging's downward movement in relation to the foot wall, the faults were typical faults (Plate III). Earth movement has caused large displacement along faults because they are planar fissures or discontinuities in rocks. Plate tectonic processes cause massive faults in the earth's crust, the largest of which constitute the borders between the plates (Ekwueme, 1993).

Plate III: Fault in the s area

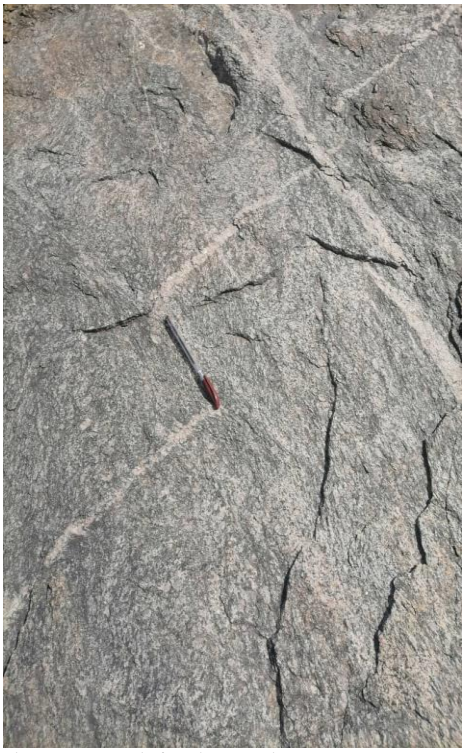

Plate IV: Fault in the study area

Dykes/veins/Alterations

When hydrothermal solution seeps through fractures, they are created. Quartz veins are found across the terrain, especially at shear zones and the interface between phyllite and dyke. They are frequently seen filling secondary material. By examining the cross-cutting relationship between the quartz veins, one can ascertain the emplacement history and time. In the western portion, the vein is primarily widely distributed, filling in weak zones that run parallel to and perpendicular to the direction of the foliation. Vein thickness varies, ranging from a few centimetres to ten metres. N20^{o}E N60^{o}W, N10^{o}E N20^{o}E, E-W, and NE-SW strikes are where these veins and veinlets are primarily oriented. They dip vertically to sub-vertically to the northern, western, and western portions, respectively. There are two types of quartz veins in the research area: smoky quartz veins and pure quartz veins, which are both white in colour. Granite, pegmatite, aplite, and dolerite lithologies were identified in the region's veins and dykes. They exhibit a variety of orientations, which correspond to the tectonic events that governed their emplacement. Rocks are well exposed in the northern portion of the study region, which is home to the majority of the mapped dykes. The gneissic rock at Mayo Sirte is penetrated by a fine-grained basaltic dyke that strikes N20^{O}E, has an exposed width of about 37 cm, and dips 50^{o}W. A quartzo-feldpartic dyke with a strike angle of 90°, an exposed length of 100 m, a width of roughly 20cm, and a vertical dip is located east of Mayo Sirte. A similar dyke, which may be a continuation of the former with comparable lithological and structural features, was discovered and extended for 7m eastward. Most of the visible Aplite veins and pegmatite dykes trend NE-SW.

Sericitization, oxidation, kaolinization, silicification, ferruginization, and other mineral-related changes are frequently linked to intense hydrothermal activity. In quartz veins found in both slate phyllite rock and felsic metavolcanic rock in the western and central regions of the study area, oxidation-type alteration is frequently observed. Oxidation is available in the following colours: yellow, reddish brown, black, light reddish, and deep reddish brown. The

oxidation or leaching of iron-bearing and vein-type iron-bearing minerals has produced the different colours.

Foliation/cleavage

There was strong foliation in the migmatite-gneiss and granite country rocks. The research area's foliation orientations range from N-S, which has a vertical dip in the northeast, to NE-SW, which has a 50° NE dip. Planar foliation was discovered in the gneiss at Mayo Sirte. The directions of the mineral alignment on the plutonic rock (granites) range from NE-SW, N-S, to NW-SE. At gneiss-dominated Gembu Hill, the lithological layering of the rocks is defined by foliation. Foliation was found wrapping around sigmoid-shaped mafic (amphibolite) xenoliths towards the northern limit at Maisamari. At the mesoscopic level, foliation wraps around the xenolith to form a pressure shadow structure. Highly worn gneiss outcrops can be found northwest of Lading. The horizontal foliation of this rock strikes at 160°. Additionally, in this region exist outcrops of worn granite with foliation (attitude: 90°, 20°S). The main trend that can be seen is N-S, according to research on foliation, cleavage, and mineral orientation. An E-W operating maximum primary stress will generate this trend in a co-axial deformation. According to Bassey (2005) and Udensi *et al*. (2003), the foliated rocks were most likely compressed in an E-W direction during the Pan-African orogeny, which is recognised as the most prominent compression episode in the Pan-African Mobile Belt.

Table 2: Some attitudes of joints taking in the study area

S/N	STRIKE	DIP
1	070	40SE
2	072	60SE
3	070	40SE
4	078	50SE
5	060	46SE
6	048	60SE
7	070	38SE
8	078	60NW
9	074	72NW
10	072	64SE
11	078	60SE
12	336	66SE
13	334	80SE
14	340	70SE
15	338	60SE
16	078	45SE
17	068	40NW
18	070	30SE
19	078	40SE
20	076	20SE
21	060	10SE
22	058	25SE

Lineaments Extracted from field measurements

With dominant dips of 31° to 40°, the lineament map created from the area's fractures shows that the NE-SW is the primary structural trend, with minor components in the NNE-SSW, ENE-WSW, and NNW-SSE, and to a lesser extent, the E-W (Figure 8), which corresponds with the trend obtained from satellite measurement (Figure 5). The findings also indicate that the structures range in size from less than two kilometres to more than ten kilometres, with the latter being limited as significant faults. These trends are similar to those discovered by Bassey *et al*. (2006) in certain areas of the northeastern sector of the Nigerian basement complex as well as those discovered using field measurements.

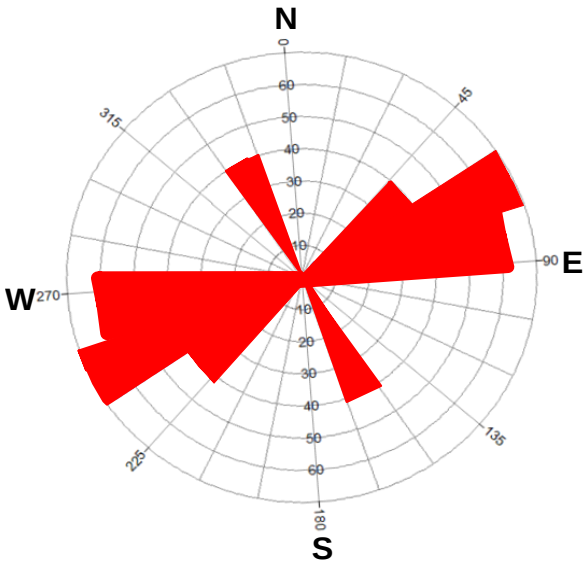

Figure:8 Rose diagram from field measurements.

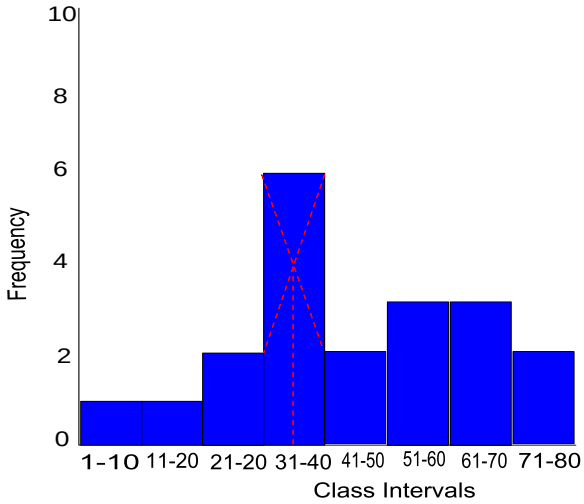

Figure:9 Histogram showing dominant dip of joints in the study Area

Artisanal Mining and Placer Deposits Around Mambilla and Environs

Surface displays of Water travels great distances in the intermittent rivers and at any time in the perennial rivers due to the significant panneling of mineralization in the area's alluvial (stream sediment) and elluvial (soil) placer deposits during the wet season. This has direct bearing on the mineral occurrence in the research region, which is located in the shear zone where hydrothermal activity is present. The locations of Maisamari, Gurgu, Yelwa, Mayo Ndaga, Lekitaba, and Nguroje are the most frequented artisanal mining sites. Gemstones, primarily blue sapphire and topaz, are among the minerals mined; amethyst and garnet are also infrequently found. Placer deposits of the minerals can be found in the beds of old rivers. Before being deposited in the current environment, the minerals were first worn from the host rocks, eroded, transported, and sorted. Afterwards, a massive overburden accumulated over them. According to Linn *et al*. (2012), these minerals are extracted from placer or secondary deposits that are connected to quartz and pegmatitic veins that intrude granitic rocks, including granites and their volcanic and subvolcanic counterparts. The predominant constituents of the alluvial deposits in the region are typically quartz, feldspars, and mica, with trace amounts of heavy minerals such iron, zircon, rutile, tourmaline, garnet, epidote, chromium spinel, sapphire, and minerals containing fluorine. There are reports of mineralizations occurring all over the world, particularly in regions with thickened continental crust or in intra-cratonic environments (Meinhold *et al*., 2015). These uncommon metal-hosting granites, associated with orogenic bands like the Central African Fold Belt, are abundant throughout the African continent (Melcher *et al.,* 2015). These nations are appropriate hosts for some mineralization since this fold belt stretches from the Gulf of Guinea to Cameroon, Nigeria, the Cantral African Republic (C.A.R.), and Sudan. Unexplored are the geochemical markers connected to these events that can help us comprehend the mineralization in the area. These crystal imprints are diagnostic features used to express transport mechanisms as interpreted to represent recently liberated grains from the source rock or suggest a relatively short transport distance (Tchunte *et al*., 2018; Ngouabe *et al*., 2022). The majority of the mineral grains from these localities have irregular morphologies. The shape of the grains changes gradually during stream transportation, becoming semispherical and angular. Long distances of transportation are reflected in the regular and semispherical grain forms (Tchunte *et al*., 2018; Ngouabe *et al*., 2022). The grains' surface texture is then altered, changing from rough and pitted to smooth. The energy and sediment composition of the stream determine all these characteristics (Fletcher and Loh, 1996a).

Results Integration

Several GIS layer methodologies, outputs, and band ratio data were integrated in order to investigate the structural tendencies that may have potential for mineralization. Based on each layer's relative suitability for the variables influencing mineralization, a classification was made. For example, a spectrum of colours (Figure 7) reflecting multi-probability (from high to low) ineralization helped to identify the structural density. The hydrothermal fluids' flow is reinforced by shear, faults, and/or fracture zones, which are places of great structural complexity. The density map of intrusion enhancement that was produced is shown in Figs. 2 and 3. It is also divided into several classes of weak points where hydrothermal solutions could potentially infiltrate. Areas with medium to high levels of intrusion are represented by yellow to orange tones, whilst low-probability regions are represented by blue.

The regions that were obtained by applying band ratios 6/7, 6/5, and 5 in RGB and signed in yellow to orange colour (Fig. 2 and 3) and characterised by an abundance of hydrated alteration minerals (such as sericite, quartz, and lithium minerals) are also nearly identical to

the locations of alteration minerals that were inferred using the technique. The optimal locations for mineralizing were predicted using the ensuing density maps (Figure 7).

The final picture of prospective mineralisation (Figure 7) was created by merging the method results with the changed zones that occurred, indicating places with high potential for mineralising. As seen in Fig. 7, the study region was split into two groups, from very low to very high, based on the number of structures present and their potential for mineralization.

There is a very excellent match between the pre-existing artisanal mines and the higher classes of the predictive areas, which is the outcome of projecting the known mining sites in the study area to validate the predictive map. In a similar vein, the remaining higher categories would indicate extremely attractive regions for possible mineralization (Figure 7). This allows for the identification of hydrothermal alteration zones by allocating the necessary funds and time for field research. The study's methods are effective at identifying the modification zones' spatial distribution, as demonstrated by the results, and as such, they can be applied to research in other comparable regions.

CONCLUSION

Combining field measurements with remote sensing data proved to be a low-cost, precise, and effective way to identify mineralization opportunities worth exploring further. In order to validate the existing artisanal mines and locate additional zones with significant mineralization potential, enhancing techniques including band ratios and remote sensing data were employed in conjunction with intrusion density maps, field measurements of structures, and structural complexity maps. The improved methods were used to identify the high structural complexity, such as shear zones, which support the motion of the hydrothermal fluid, using satellite data and site field observations. On the other hand, based on the spectral fingerprints of certain minerals, band ratios and the field technique identified alteration zones.

A significant NE-SW shear zone and less frequent NNW, WNW, NS, and NE trends indicate zones of high structural density in the structural and lineament density map that was generated from field measurements and remote sensing data. Furthermore, when the predicted map was validated using published structural data from a few known artisanal mine sites in the research area, a significant degree of similarity was noted. Thus, combining the site geological data with the images data acquired from satellites shows promise for discovering a fresh potential that may be used for further exploration.

Declaration of Competing Interest

The authors declare that they have no known competing financial interests or personal relationships that could have appeared to influence the work reported in this paper.

REFERENCES

Abdelnasser, A., Kumral, M., 2017. The nature of gold-bearing fluids in Atud gold deposit, Central Eastern Desert, Egypt. Int. Geol. Rev. 59 (15), 1845–1860.

Bassey.N.E.(2005). Selective structural geological mapping and interpretation of landsat and aeromagnetic data over Hawall Basement Complex, Northeast Nigeria, Unpublished PhD thesis, Abubakar Tafawa Balewa University, Bauchi, pp209.

Buchroithner.M.F (2002) Marinko Oluić: Earth Imaging and Exploration from Space: Satellit es Sensors –Applications *Geodetski List, Zagreb, Croatia* 56: 68-69

Carper, W,J., T.M. Lillesand, and R.W. Kiefer, (1990). The use of intensityhue-saturation transformations for merging SPOT panchromatic and multispectral data, Photogrammetric Engineering 6. Remote Sensing, 56(4):459-467.

Daily, M. I., (1975). Surface Roughness Discrimination with L-Band SLAR, Geo2ogical Society of America, Abstracts with Programs, Pullman, Washington.

Domzalski, W., 1964. Importance of aeromagnetics in evaluation of structural control of mineralization. Geophys. Prospecting 14 (3), 273–291.

Dupreez.J.W, Barber W (1965). The distribution and chemical quality of ground water in Northern Nigeria. Bulletin 36. Geological survey of Nigeria 93.

Eldosouky, A.M., 2019. Aeromagnetic data for mapping geologic contacts at Samr El- Qaa area, North Eastern Desert, Egypt. Arab. J. Geosci. 12, 2.

Ekwueme,B.N. (1993):An easy approach to igneous petrology University of Calabar Press pp 19-153.

El-Shazly, A.K., Khalil, K.I., 2014. Banded iron formations of Um Nar, Eastern Desert of Egypt: P-T–X conditions of metamorphism and tectonic implications. Lithos,Volumes 196-197, 356–375.

Farrand, W.H., Harsanyi, J.C., 1997. Mapping the distribution of mine tailings in the Coeur d'Alene River Valley, Idaho, through the use of a constrained energy minimization technique. Remote Sens. Environ. 59, 64–76.

Franklin, S.E and F. Blodgett.C.F(1993). An example of satellite multisensor data fusion, Computers & Geosciences, Volume 19, Issue 4, Pages 577-58.

Ganas, A., Pavlides, S., Karastathis, V., 2005. DEM-based morphometry of rangefront escarpments in Attica, central Greece, and its relation to fault slip rates. Geomorphology 65 (3-4), 301–319.

Geomatics(PCI) Enterprises Inc, 2015. geospatial image processing software. www.pcigeomatics.com..

Goetz, A.F.H., Rock, B.N., Rowan, L.C., 1983. Remote sensing for exploration: an overview, Econ. Geol. 78, 573-590.

Helmy, M., Reinhard, K., Fritz, H., Loizenbauer, J., 2004. The Sukari Gold Mine, Eastern Desert-Egypt: structural setting, mineralogy and fluid inclusion study.Mineral. Deposita 39, 49.

Jeje L.K (1983). Aspects of geomorphology of Nigeria. Heinemann educational books.

Klemm, R., Klemm, D., 2013. Gold and gold mining in anceint Egypt and Nubia. Springer. https://doi 10.1007/978-3-642-22508-6.

Linnen, R.L., Van Lichtervelde, M.., & ˇCerný, P. (2012). Granitic pegmatites: Granitic pegmatites as sources of strategic metals. Elements 2012, 8, 275–280.

Melcher, F., Graupner, T., Gabler, H.E., Sitnikova, M., Henjest-Hunst, F., Orberthur, T., Gerdes, A., Dewaele, S. (2015). Tantalum (niobium-tin) mineralization in Africa pegmatites and rare-meta granites. Constraints from Ta-Nb oxides mineralogy, geochemistry and U-Pb geochronology. Ore Geo. Rev. 64, 667- 719.

Meinhold, G., Andres, B., Kostopoulos, D. and Reischmann, T. (2008). Rutile Chemistry and Thermometry as Provenance Indicator: An Example from Chios Island, Greece. Sedimentary Geology, 203, 98-111. https://doi.org/10.1016/j.sedgeo.2007.11.004.

Mould .A.W. S (1960). Report on a rapid reconnaissance soil survey of the Mambilla plateau. Bulletin 15, Soil survey section, regional research station, ministry of agriculture, Samaru, Zaria.

Mubi AM, Tukur. A.L (2005). Geology and relief of Nigeria. Nigeria. Heinemann educational books.

Nikolakopoulos, K.G., Kamaratakis, E.K., Chrysoulakis, N., 2006. SRTM vs ASTER elevation products. Comparison for two regions in crete, Greece. Int. J. Remote Sens.. 27 (21), 4819–4838.

Ngouabe, E.G.T., Vishiti, A., Nforba, M.T., Etame, R.S.J · Cheo Emmanuel Suh, C.E. (2022). Morphology and composition of alluvial gold from theMeiganga area, northern Cameroon: implications for provenance. Journal of Sedimentary Environments https://doi.org/10.1007/s43217-022-00115-5.

Papathanassiou,K.P and Buchroithner,M.F (1993). Signature Analysis of Multifrequency Polarimetric NASA DC-8AIRSAR Data for Alpine Geo-Applicatios *EARSel Advances in Remote Sensing, Neapel, Italy* 2: 1. 287-299

Pradhan, B, Lee, S and Buchroithner , M F (2010) .Remote sensing and GIS-based landslide susceptibility analysis andits crossvalidation in three test areas using a frequency ratio model *Photogrammetrie Fernerkundung Geoinformation (Accepted: to be published in vol. 1, 2010)*

Pradhan.B, Lee.S,Mansor.S, Buchroithner.M.F, Jamaluddin.N, Khujaimah.Z (2008) .Utilizatio n of optical remotesensing data and geographic information system tools for regional landslide hazard analysis by usingbinomial logistic regression model *Journal of Applied Remote Sensing* 2: 1-11.

Pour, A.B., Hashim, M., Hong, J.K., Park, Y., 2019. Lithological and alteration mineral mapping in poorly exposed lithologies using Landsat-8 and ASTER satellite data: north-eastern Graham Land, Antarctic Peninsula. Ore Geol. Rev. 108, 112–133.Ramadan.

Roy, D.P., Wulder, M.A., Loveland, T.R., C.E., W., Allen, R.G., Anderson, M.C., Helder, D., Irons, J.R., Johnson, D.M., Kennedy, R., Scambos, T.A., Schaaf, C.B., Schott, J.R.Sheng, Y., Vermote, E.F., Belward, A.S., Bindschadler, R., Cohen, W.B., Gao, F., Hipple, Hostert, P., Huntington, J., Justice, C.O., Kilic, A., Kovalskyy, V., Lee, Z.P., Lymburner, L., Masek, J.G., McCorkel, J., Shuai, Y., Trezza, R., Vogelmann, J., Wynne, R.H., Zhu, Z., 1998. Landsat-8: Science and product vision for terrestrial global change research. Remote Sens. Environ. 145, 154–172.

Süzen, M.L., Toprak, V., 1998. Filtering of satellite images in geological lineament analyses: an application to a fault zone in Central Turkey. Int. J. Remote Sens. 19(6), 1101–1114.

Tchunte, P.M.F., Tchameni, R, André-Mayer, A.S., Dakoure, H.S., Turlin, F., Poujol, M, Nomo, E.N., Fouotsa, A.S.F., Rouer, O. (2018). Evidence for Nb-Ta Occurrences in the Syn.Tectonic Pan-African Mayo Salah Leucogranite (Northern Cameroon): Constraints from Nb-Ta Oxide Mineralogy, Geochemistry and U-Pb LA-ICP-MS Geochronology on Columbite and Monazite. doi:10.3390/min8050188.

Tukur, A. L, Adebayo. A. A, Galtima A (2005). The land and people of the Mambilla Plateau, Nigeria. Heinemann educational.

Udensi, E. E., Osazuwa I. B. and Daniyan, M. A. (2003). Trend analysis of the total magnetic field over the Bida Basin, Nigeria. Nigerian Journal of Physics. 15,143–151.